Predicting the ripening of papaya fruit with digital imaging and random forests

Article *in* Computers and Electronics in Agriculture · February 2018

DOI: 10.1016/j.compag.2017.12.029

CITATIONS
26

READS
1,872

4 authors:

Luiz Pereira
University of Campinas
1 PUBLICATION **26** CITATIONS
SEE PROFILE

Sylvio Barbon
Universidade Estadual de Londrina
143 PUBLICATIONS **591** CITATIONS
SEE PROFILE

Nek Valous
National Center for Tumor Diseases (NCT) Heidelberg
98 PUBLICATIONS **910** CITATIONS
SEE PROFILE

Douglas F Barbin
59 PUBLICATIONS **1,352** CITATIONS
SEE PROFILE

Computers and Electronics in Agriculture 145 (2018) 76–82

Contents lists available at ScienceDirect

Computers and Electronics in Agriculture

journal homepage: www.elsevier.com/locate/compag

Original papers

Predicting the ripening of papaya fruit with digital imaging and random forests

Luiz Fernando Santos Pereira[a], Sylvio Barbon Jr.[b,*], Nektarios A. Valous[b], Douglas Fernandes Barbin[a]

[a] Department of Food Engineering, University of Campinas, Brazil
[b] Department of Computer Science, Londrina State University (UEL), Londrina, Brazil

ARTICLE INFO

Keywords:
Image analysis
Machine learning
Classification
Computer vision
Maturation stage

ABSTRACT

Papaya grading is performed manually which may lead to misclassifications, resulting in fruit boxes with different maturity stages. The objective is to predict the ripening of the papaya fruit using digital imaging and random forests. A series of physical/chemical analyses are carried out and true maturity stage is derived from pulp firmness measurements. Imaging and image analysis provides hand-crafted color features computed from the peel and random decision forests are implemented to predict ripening stage. More specifically, a total of 114 samples from 57 fruits are used for the experiments, and classified into three stages of maturity. After image acquisition and analysis, twenty-one hand-crafted color features (comprising seven groups) that have low computational cost are extracted and evaluated. Random forests with two datasets (cross-validation and prediction set) are employed for the experiments. Concerning all image features, 94.3% classification performance is obtained over the cross-validation set. The prediction set obtained 94.7% misclassifying only a single sample. For the group comparisons, the normalized mean of the RGB (red, green, blue) color space achieved better performance (78.1%). Essentially, the technique can mature into an industrial application with the right integration framework.

1. Introduction

Papaya is a berry fruit with high nutritional and commercial value due to its non-seasonality and reduced time to harvest. In 2013, the world production of papaya reached 1.25×10^7 mt (Faostat, 2016). Papaya grading (as carried out in packing houses) is performed manually by human operators which may lead to misclassifications, resulting in fruit boxes with different maturity stages (Savakar and Anami, 2015). Visual inspection has been serving the fruit industry for many years, but it may lead to inconsistencies and variations despite the professional training of the graders. The variability associated with human assessment pertinent to automated inspection tasks accentuates the need for objective measurement systems providing reliable information throughout production (Damez and Clerjon, 2008). However, this must not sacrifice the essential benefits of human grading, e.g. intuition (Valous et al., 2016).

The identification of ripening stage is important, as it is related to internal properties of the fruit such as sweetness and firmness (Magwaza and Opara, 2015). In addition, it helps to determine storage time prior to consumption. The determination of these properties is carried out by analytical techniques commonly used for agricultural products. These techniques are time-consuming and destructive, plus they usually require chemical reagents and lengthy sample preparation procedures. In addition, they are applied to a limited number of samples which are not representative of the typical physico-chemical variability found in such batches. Thus, rapid, intelligent, and non-destructive techniques are required in this application domain (Wu and Sun, 2013).

Computer vision systems have been used for agri-food quality evaluation and control (Jackman et al., 2012). Quality assessment can be performed by such systems and is based on consumer digital cameras which are widely available. This approach has several advantages: rapid time of analyses, low cost, high accuracy and precision. For example, in a study researchers extracted color features to predict the ripening of stone fruits with low misclassification rates (Eyarkai Nambi et al., 2016). In addition, researchers applied laser-induced fluorescence spectroscopy to classify papaya into four quality grades (Obledo-Vazquez and Cervantes-Martínez, 2017a). It is reported that this technique is able to distinguish between ripe and unripe fruits from fluorescence measured at 690 and 740 nm. However, the study has a small

* Corresponding author.
E-mail addresses: barbon@uel.br (S. Barbon), dfbarbin@unicamp.br (D.F. Barbin).

https://doi.org/10.1016/j.compag.2017.12.029
Received 22 August 2017; Received in revised form 12 December 2017; Accepted 18 December 2017

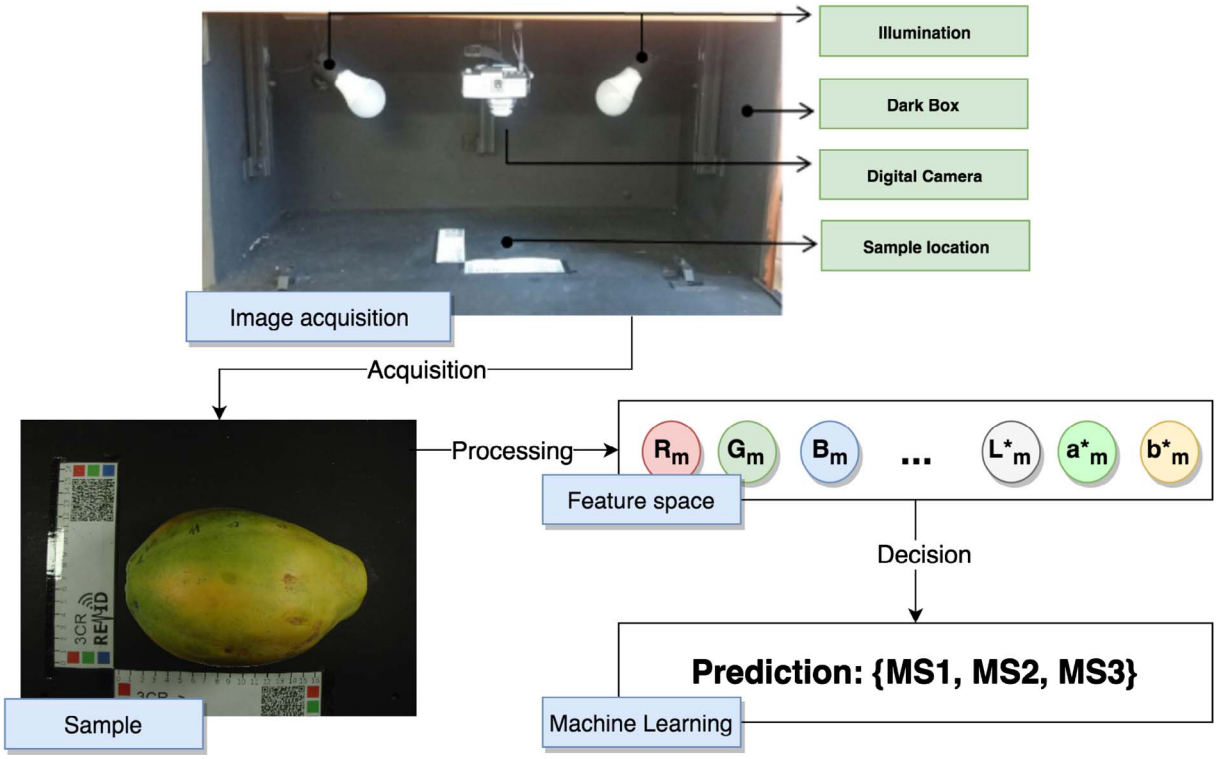

Fig. 1. Overview of image acquisition, feature computation, and final prediction workflow for assessing the ripening of the papaya fruit.

amount of samples and a full classification model is not reported. In addition, the region between 690 and 740 nm is in the visible range of the electromagnetic spectrum. Practically, digital imaging systems may be the simpler approach for predicting maturity stages in papaya.

Machine learning techniques are being used in a variety of domains (Ropodi et al., 2016). The application of these techniques in agri-food characterization and evaluation has been also investigated (Wang et al., 2012; Liu et al., 2013; Papadopoulou et al., 2013; Prevolnik et al., 2014). Random decision forests, support vector machines, as well as miscellaneous types of artificial neural networks are implemented in many studies related to agri-food quality evaluation (Granitto et al., 2007; Chen et al., 2010; Valous et al., 2010; Wang et al., 2012; Papadopoulou et al., 2013; Liu et al., 2013; Savakar and Anami, 2015; Muñoz et al., 2015; Rojas-Moraleda et al., 2016; da Costa Barbon et al., 2017). In general, the literature has been reporting comparisons between conventional machine learning methods in various research domains, since there seems to be no clear consensus on absolute winners. On the other hand, an extensive benchmarking report demonstrated that random decision forests (RF) as an ensemble learning method (Breiman, 2001) may provide equal or better performance when compared to other classification algorithms (support vector machines, C4.5, AdaBoost, k-nearest neighbours, logistic regression, stochastic gradient boosting trees, extreme learning machines, sparse representation-based classification, and deep learning) on publicly available datasets (Zhang et al., 2017). For example, researchers compared random forests with neural networks and support vector machines for electronic tongue data classification, with RF achieving 99.07% accuracy (Liu et al., 2013). In another study, RF provided a measure of variable importance in clustering when investigating the similarity of six vegetable oils (Ai et al., 2014). Yet in another example, RF models gave an estimation of the relative importance of each sensory attribute for the discriminant function (Granitto et al., 2007). Finally, in Barbon et al. (2016) RF demonstrated superior prediction results in identifying pork storage time compared to artificial neural networks, fuzzy-based classifiers, support vector machines, *k*-nearest neighbours, and decision trees.

Hence, the aim of this work is to predict the ripening of the papaya fruit using digital imaging and random forests. A series of physical/chemical analyses are carried out and true maturity stage is derived from pulp firmness measurements. Imaging and image analysis provides hand-crafted color features computed from the peel and random decision forests are implemented to predict ripening stage.

2. Material and methods

2.1. Experimental design

Fifty-seven golden papaya fruits were purchased in a retail market in the city of Campinas (Brazil). Two color images per sample were acquired (one from each side) and physical/chemical analyses (pulp firmness, pH, soluble solids, total carotenoids, and ascorbic acid content) were carried out. All samples were classified into three maturity stages: maturity stage 1 (MS1; 58 images), maturity stage 2 (MS2; 30 images), and maturity stage 3 (MS3; 26 images). There were differences in the number of samples from each maturity stage because samples were collected and initially classified visually. Later on, the fruits were classified according to pulp firmness scores. Fruits with pulp firmness > 33 N were classified as MS1. Samples graded as MS2 had pulp firmness < 33 N and > 20 N, and fruits graded as MS3 had pulp firmness < 20 N. Pulp firmness is considered an important trade property since edible fruits should have pulp firmness < 20 N (Blankenship and Unrath, 1988; Kim et al., 1999).

2.2. Image acquisition

Images were acquired by a computer vision system consisting of three main components: an illumination source, a consumer digital camera, and a rectangle box with matte black internal walls to avoid specular reflections (Fig. 1). The lighting system consists of LED lamps (Natural daylight, 100 W). The camera (Sony, Japan) is located vertically over the background at a distance of 17.5 cm from the sample. The camera is mounted on a stand, which allows easy vertical movement and stable support, and connected to the USB port of a workstation to

acquire and visualize the images. The angle between the camera lens and lighting source axis is approx. 45°. Images are acquired using the following camera settings: manual exposure with shutter speed of 1/60 s (zoom and flash functions off) and ISO number of 200.

2.3. Physical/chemical analyses

Fruit length and diameter were measured by a digital caliper (Mitutoyo, Japan). The samples were weighed using a digital analytical balance (Gehaka BG, Brazil) with precision of ± 0.01 g. Peel color was measured by a colorimeter (HunterLab, USA). Pulp firmness was measured with a texturometer (Stable Micro Systems, UK) using a stainless steel probe with a diameter of 6 mm (penetration depth of 20 mm and velocity 1 mm/s); each sample was cut along the larger side and six measurements were done per fruit at three points (on each side), so the average value of the maximum rupture force represents pulp firmness. Soluble solids content (SSC) was analyzed through a digital refractometer (Atago, Japan) with automatic temperature correction (AOAC, 2005). The pH was determined with a potentiometer (Kasvi, Brazil) (AOAC, 2005). SSC and pH were represented as the average of two measurements per sample. Ascorbic acid (AA) concentration was measured using oxalic acid solution (Benassi and Antunes, 1988). The carotenoid content of the pulp was determined according to the literature (Rodriguez-Amay, 2001).

2.4. Image analysis and feature extraction

Each color image was pre-processed in MATLAB R2015a (Mathworks, USA). Color calibration was not necessary since this is not a characterization study and only color changes are sought after and quantified and not absolute color values. Pre-processing included region of interest (ROI) detection and normalization. The RGB, HSV, and CIE L*a*b* color spaces were explored in this study: red (R), green (G), blue (B), hue (H), saturation (S), value (V), L* (lightness), a* (red-green) and b* (yellow-blue) color channels, respectively. Color channels were analyzed separately and additional features were generated by normalization and area computation (Fig. 2).

ROI selection was performed with thresholding. The saturation (S) channel was used due to high contrast between the sample and background. From the binary image obtained, region growing was performed to remove redundant objects (e.g. paper ruler). In this way, only the fruit region was used for feature extraction: R_m, G_m, B_m, H_m, S_m, V_m, L^*_m, a^*_m, and b^*_m (Fig. 2). In order to obtain informative features from a color channel, the mean pixel value in a ROI was computed (Antonelli et al., 2004; Vélez-Rivera et al., 2014; Eyarkai Nambi et al., 2016). Eq. (1) was used to extract features from each color channel: R_m (red), G_m (green), B_m (blue), R_{nm} (normalized red), G_{nm} (normalized green), B_{nm} (normalized blue), H_m (hue), S_m (saturation), V_m (value), L^*_m (L*), a^*_m (a*), and b^*_m (b*):

$$MeanValue(ROI) = \frac{\sum_{x=1}^{x}\sum_{y=1}^{y} ROI_{xy}}{n} \quad (1)$$

where n is the number of pixels in the ROI and ROI_{xy} is the pixel value in the (x,y) position. As an example, in the study of Eyarkai Nambi et al. (2016), R_{nm}, G_{nm}, and B_{nm} were computed from the normalization of R, G, and B color channels to predict the ripening of mango. All color channels are normalized by $R_{nm} = R_m/(R_m + G_m + B_m)$, $G_{nm} = G_m/(R_m + G_m + B_m)$, and $B_{nm} = B_m/(R_m + G_m + B_m)$.

Additional features were obtained from the normalized color channels after thresholding R_{nm}, G_{nm}, and B_{nm}. Thus, the number of pixels inside the ROI were assigned to R_{mb}, G_{mb}, and B_{mb}, respectively. Based on these values it was possible to extract the normalized differential index (NDI) from each color channel. The NDI of R, G, and B color channels (Eqs. (2)–(4), respectively) are given by Garrido-Novell et al. (2012) and Payne et al. (2013):

$$NDI_{rg} = \frac{|R_{mb} - G_{mb}|}{R_{mb} + G_{mb}} \quad (2)$$

$$NDI_{rb} = \frac{|R_{mb} - B_{mb}|}{R_{mb} + B_{mb}} \quad (3)$$

$$NDI_{gb} = \frac{|G_{mb} - B_{mb}|}{G_{mb} + B_{mb}} \quad (4)$$

Table 1 shows the twenty-one hand-crafted color features that were computed for predicting the ripening of papaya.

2.5. Classifier setup and statistical analyses

Decision tree algorithms represent the knowledge acquired in the form of a tree, which is easy to re-write with straightforward rules. The more robust RF algorithm based on the tree ensemble is computationally efficient and operates by constructing a multitude of decision trees at training time and outputting the class that is the mode of the classes of the individual trees. Random forests grow decision trees towards classifying a new object from an input vector, going through the input vector down in all trees of the forest. The number of features in each node and the number of trees are parameters defined by the end user (Barbon et al., 2016). Each tree is induced by an out-of-bag strategy (sampling with replacement) which leaves part of the features out of the sample. This strategy allows RF to perform an unbiased estimation of the classification error and to compute the importance of the features. During prediction, a class is obtained from each decision tree (voting scheme). The algorithm chooses the classification having the most votes over all trees in the forest. Random decision forests correct for decision trees' habit of overfitting to their training set, and can address multi-class classification problems with unbalanced or small datasets without pre-processing routines (Breiman, 2001). Moreover, RF is a trustful method that always converges, avoiding the overfitting problem. In the most common RF implementation, split selection for building the decision tree is performed based on the decrease of the Gini impurity measure; this provides a relative ranking of features as described in Menze et al. (2009). Overall, RF achieves satisfactory results for food quality evaluation purposes (Granitto et al., 2007; Liu et al., 2013; Ai et al., 2014; Barbon et al., 2016).

Therefore, a solution was implemented in the R language v.3.3.1 using the `randomForest` library with 500 decision trees and standard hyper-parameters. Analysis of variance (ANOVA) was performed for identifying the differences in physical/chemical properties among maturity stages using the statistical package MINITAB 14.12 (Minitab Inc, USA). In order to evaluate the model outputted by the RF algorithm, two datasets were created: cross-validation and prediction test set. The cross-validation set was used to induce the models toward adjusting the hyperparameters (30 iterations), while the prediction test set was employed to evaluate classification performance. This division was made in order to minimize the risks of overfitting by means of the Kennard-Stone algorithm (Kennard and Stone, 1969).

3. Results and discussion

3.1. Analysis of physical and chemical properties

No statistical differences were observed ($p < 0.05$) in the dimensions and masses among samples coming from the three maturity stages (Table 2). Thus, peel appearance and color account for the visual differences among samples. In this regard, internal properties such as soluble solids content and pulp firmness become important parameters for determining ripeness, since the consumer will search for attributes such as sweetness and texture. Hence, internal properties were determined and analyzed according to each maturity stage (Table 3).

Essentially during ripening, there is a transformation of acids into sugars (Obledo-Vazquez and Cervantes-Martínez, 2017b). Although an

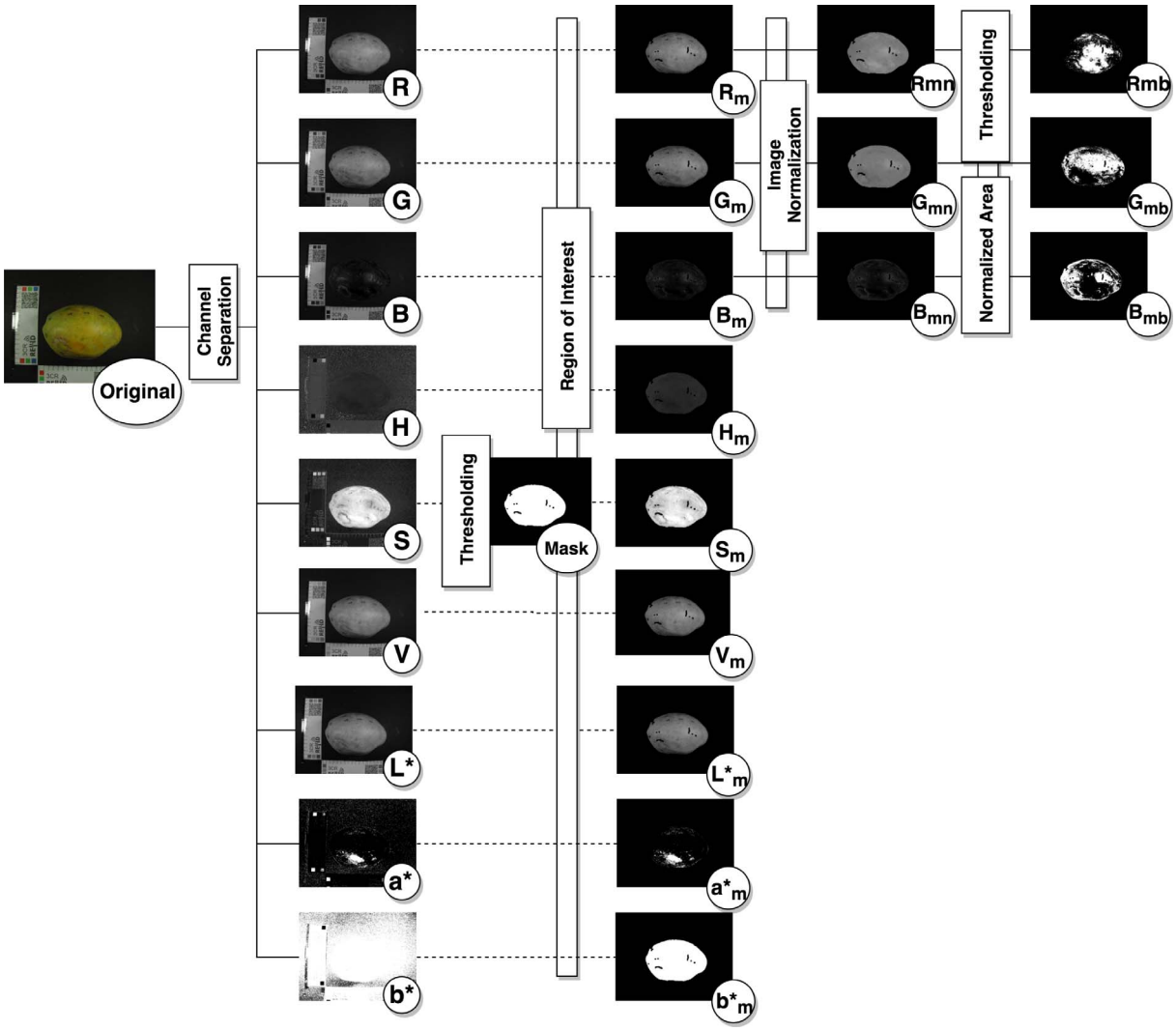

Fig. 2. Overview of the image analysis and feature extraction pipeline.

Table 1
List of hand-crafted color features for ripening prediction.

No.	Name	Description
1	R_m	Mean value of the R channel (Eq. (1))
2	G_m	Mean value of the G channel (Eq. (1))
3	B_m	Mean value of the B channel (Eq. (1))
4	R_{nm}	Mean value of normalized R channel (Eq. (1))
5	G_{nm}	Mean value of normalized G channel (Eq. (1))
6	B_{nm}	Mean value of normalized B channel (Eq. (1))
7	R_a	Area of the R channel
8	G_a	Area of the G channel
9	B_a	Area of the B channel
10	R_{na}	Area of normalized R channel
11	G_{na}	Area of normalized G channel
12	B_{na}	Area of normalized B channel
13	NDI_{rg}	Normalized differential index of red to green (Eq. (2))
14	NDI_{rb}	Normalized differential index of red to blue (Eq. (3))
15	NDI_{gb}	Normalized differential index of green to blue (Eq. (4))
16	H_m	Mean value of the H channel (Eq. (1))
17	S_m	Mean value of the S channel (Eq. (1))
18	V_m	Mean value of the V channel (Eq. (1))
19	L^*_m	Mean value of the L* channel (Eq. (1))
20	a^*_m	Mean value of the a* channel (Eq. (1))
21	b^*_m	Mean value of the b* channel (Eq. (1))

Table 2
Length, diameter, and mass data for each ripening stage.

Maturity stage	Dimensions		Mass (g)
	Length (cm)	Diameter (cm)	
MS1	13.83 ± 0.93^a	8.94 ± 0.56^a	534.95 ± 95.98^a
MS2	13.82 ± 0.92^a	8.86 ± 0.39^a	519.18 ± 51.72^a
MS3	13.96 ± 1.10^a	8.66 ± 0.56^a	499.40 ± 89.70^a

Mean ± st. dev. values in same column denoted by same letter do not differ statistically ($p < 0.05$, Tukey's honest significance test). MS1: maturity stage 1, MS2: maturity stage 2, and MS3: maturity stage 3.

increasing trend is observed in the soluble solids content with ripening, no significant differences are observed for samples in different maturity stages. Papaya should have a minimum of 11.50° Brix for marketing purposes (Zhou and Paull, 2001; Bron and Jacomino, 2006). In the current study, low values of soluble solids were found for some fully mature fruits (MS3) (Table 3). This indicates that fruits with yellow peel color still have a low amount of soluble solids. Furthermore, the maximum value of soluble solids for MS1 is 13.93° Brix demonstrating that fruits with green peel already have a high amount of soluble solids. Ascorbic acid, pH, and carotenoids were not significantly different ($p < 0.05$) among the three maturity stages.

Regarding pulp firmness, a high standard deviation for MS1

Table 3
Physical/chemical analyses and peel color data for each ripening stage.

Physical/chemical analysis	Maturity stage	Min	Max	Mean
Soluble solids (Brix)	MS1	6.93	13.93	11.67(±1.77^a
	MS2	11.57	13.43	12.68 ± 0.55^a
	MS3	10.60	13.40	12.14 ± 0.91^a
Pulp firmness (N)	MS1	7.53	93.56	43.9 ± 25.4^a
	MS2	10.59	35.08	19.4 ± 9.0^b
	MS3	1.31	19.19	9.1 ± 5.3^b
Moisture (%)	MS1	0.86	0.91	0.88 ± 0.01^a
	MS2	0.86	0.92	0.88 ± 0.02^a
	MS3	0.87	0.92	0.88 ± 0.01^a
pH	MS1	5.60	6.04	5.84 ± 0.13^a
	MS2	5.59	5.98	5.81 ± 0.13^a
	MS3	5.56	5.91	5.77 ± 0.10^a
Ascorbic acid (mg/100 g)	MS1	59.37	140.52	98.4 ± 19.1^a
	MS2	63.08	128.73	101.5 ± 15.9^a
	MS3	59.37	139.98	92.1 ± 28.6^a
Carotenoids (μg/g)	MS1	9.18	23.03	16.5 ± 4.1^a
	MS2	6.54	26.95	17.2 ± 5.4^a
	MS3	7.38	21.78	15.3 ± 3.3^a
Peel color				
L* (lightness)	MS1	44.92	60.20	55.66 ± 3.01^b
	MS2	54.95	68.58	61.09 ± 3.41^a
	MS3	55.44	67.16	62.08 ± 3.32^a
a* (green-red)	MS1	−10.06	−1.25	−5.01 ± 2.08^b
	MS2	−2.30	4.26	1.48 ± 2.26^a
	MS3	−2.46	8.29	2.87 ± 3.68^a
b* (blue-yellow)	MS1	27.45	44.92	39.14 ± 3.60^b
	MS2	38.21	51.44	45.54 ± 4.42^a
	MS3	42.53	55.12	49.01 ± 3.95^a

Mean ± st. dev. values in same column denoted by same letter do not differ statistically ($p < 0.05$, Tukey's honest significance test). MS1: maturity stage 1, MS2: maturity stage 2, and MS3: maturity stage 3.

(coefficient of variation 25%) and a clear decreasing trend during ripening were observed. Papaya should have optimally pulp firmness values < 20 N for consumption (Blankenship and Unrath, 1988; Kim et al., 1999). The results indicate that (in average) samples from MS2 also had values < 20 N, thus suitable for purchasing. In addition, some fruits from MS1 have pulp firmness values < 20 N; since samples were classified based on this particular property, this indicates that parts of the fruits are soft although the average value is still high.

Regarding peel color, statistical differences were observed ($p < 0.05$) between fruits graded as MS1 and those graded as MS2 and MS3. In order to obtain a representative color profile, the fruit surface should be relatively uniform or homogeneous (Kang et al., 2008) but still a higher number of colorimetric measurements is required (O'Sullivan et al., 2003; Nagle et al., 2016). Essentially, a digital imaging system is advantageous since it provides information from the fruit surface as a whole, as opposed to the small regions measured by the colorimeter.

3.2. Performance of hand-crafted color features

RF models were tested for maturity stage (Fig. 3) prediction over the two datasets. After 30 iterations with all hand-crafted features (Table 1), an average performance of 94.3% ± 0.01 (st. dev.) was reported for the cross-validation set. The predictive accuracy for MS1 was 95.4% ± 0.00. Results for MS2 and MS3 were 92.1% ± 0.02 and 84.4% ± 0.02, respectively. A box plot (Fig. 4) allows to observe the flat appearance of MS1 and MS2 due to the small standard deviation. On the other hand, MS3 has an irregular quartile distribution. This confirms that MS3 is more difficult to classify compared to the other classes.

Independent of maturity stage, some fruit samples are incorrectly predicted at least in one iteration (Table 4). It is important to highlight that all misclassified samples are wrongly predicted by just one maturity stage considering both datasets. From the cross-validation set, samples #42, #56, #66, and #87 were reported as misclassified. Sample #111, the only misclassified sample from the prediction set, is actually classified as MS3 but predicted as MS2.

Considering the prediction set, MS1 and MS2 were correctly predicted (100% accuracy). However, MS3 obtained 80%. In Fig. 5 it is possible to observe the color heterogeneity of the peel for this particular sample (#111), which may be a cause for the erroneous predictions. Doubts about the predicted maturity stage can arise when classification is performed using the peel color information only. Thus, for some fruits the direct link between surface color and internal properties may not be valid; these fruits have a green peel with high amount of soluble solids and low values of pulp firmness. In addition, fruits that are firm and have low amount of soluble solids, have a yellow peel; these samples can also be erroneously classified by techniques that use the peel color information only, including conventional visual assessments. With the number of samples already in the model a good classification accuracy was reached. However, more samples could be introduced to the model in order to enhance its applicability.

3.3. Group comparisons

The group composed of the mean values of normalized R, G, and B color channels achieved better predictions. Essentially R_{nm}, G_{nm}, and B_{nm} (NRGB in Fig. 6) achieved better results, 78.1% ± 0.03. The groups based on the average values of the R, G, and B color channels (R_m, G_m and B_m) showed satisfactory accuracy (RGB in Fig. 6) obtaining 65.1% ± 0.01. Simple average values of color channels achieved good results with CIE L*a*b* (L^*_m, a^*_m, and b^*_m) predicting the maturity stage at 70.1% ± 0.01. Results obtained by the RGB normalized differential index were not so accurate (50.8% ± 0.03), HSV (H_m, S_m, and V_m) had

(a) MS1 (b) MS2 (c) MS3

Fig. 3. Sample images from each maturity stage of the papaya fruit. The three maturity stages MS1, MS2, and MS3 are derived from pulp firmness measurements.

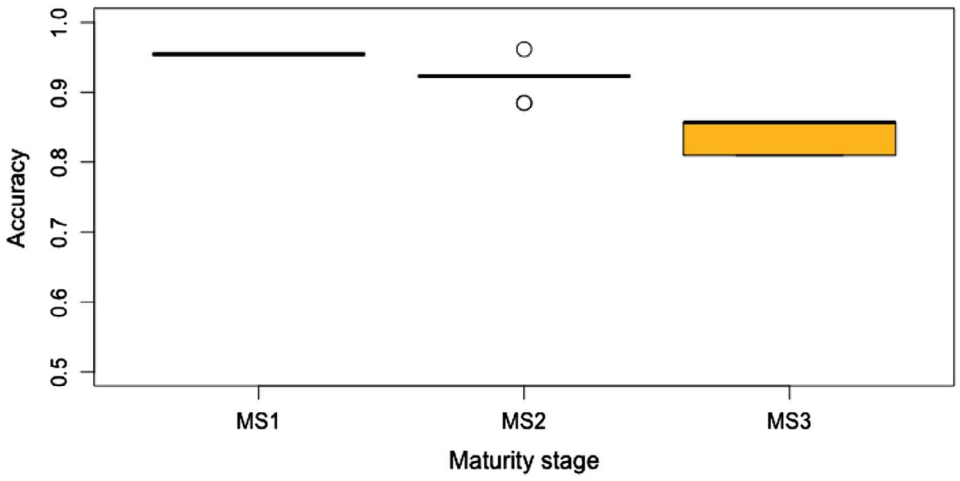

Fig. 4. Box plot showing predictive accuracy at each ripening stage for the cross-validation set; MS1 is easier to classify than MS2 and MS3.

Table 4
Misclassified samples occurring at least once during classification over both datasets.

Samples #	Cross-validation				Prediction
	42	56	66	87	111
Maturity stage (true)	1	2	2	3	3
Maturity stage (predicted)	2	3	3	2	2

an accuracy of 57.3% ± 0.03, and the image descriptors based on area (normalized RGB area) had 35.2% ± 0.04.

The results obtained using the mean values of RGB channels were similar to the classification of mangoes. A misclassification rate of 17% was reported using linear discriminant analysis and the mean of normalized pixel values for the RGB components. Classification was improved when the normalized differential index of RGB channels was used (Eyarkai Nambi et al., 2016). In comparison, the classification of apples into four groups according to color features reached 66.2% of correctly classified samples, using RGB features as predictors and linear discriminant analysis (Garrido-Novell et al., 2012). The accuracy obtained in this study corroborates the potential application of computer vision for the fast inspection of agricultural products.

4. Conclusions

Classification performance is a good measure of the reliability of the feature set. Since samples are classified based on pulp firmness, results indicate that this internal property is linked to the color of the fruit peel. Through color image processing, satisfactory results are reported for papaya grading based on pulp firmness. By combining hand-crafted image features with machine learning techniques, it is possible to reach higher accuracy and improve classification models for the papaya fruit. This particular application of computer vision could enable the development of a relatively simple and automated system to sort papaya according to different levels of maturity. Digital imaging technologies continue to change at a rapid pace and the techniques that have been developed can evolve into industrial applications with the right integration framework. Further investigation is required for achieving robust levels of ripening prediction. This can be done through more elaborate hand-crafted features and fast learning using some extreme learning machine variant, or through the use of deep learning in which directly distilling information from images allows the reduction of human bias.

5. Compliance with ethical standards

Funding: this study was funded by Sao Paulo Research Foundation (FAPESP), Young Researchers Award, Grant No. 2015/24351-2; and FAEPEX, UNICAMP, Grant No. 10316.

Conflict of interest: Luiz Fernando Santos Pereira declares that he has no conflict of interest. Sylvio Barbon Jr. declares that he has no conflict of interest. Nektarios A. Valous declares that he has no conflict of interest. Douglas Fernandes Barbin declares that he has no conflict of interest.

Ethical approval: this article does not contain any studies with human participants or animals performed by any of the authors.

Informed consent: not applicable.

(a) Original image (b) Pre-processed image

Fig. 5. Fruit sample #111 misclassified from the prediction set.

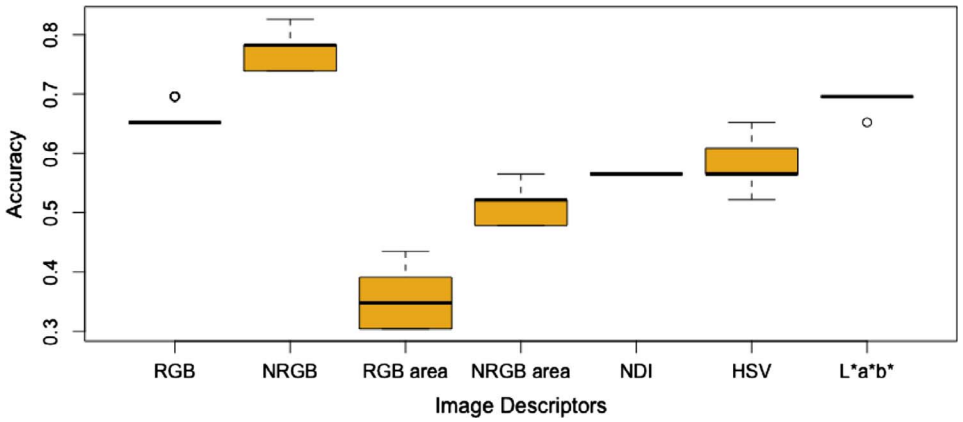

Fig. 6. Box plot showing the performance of the prediction set for the grouped features.

Acknowledgments

This research was supported by Sao Paulo Research Foundation (FAPESP), Young Researchers Award, Grant No. 2015/24351–2, and FAEPEX-Unicamp, Grant No. 10316. Luiz Fernando Santos Pereira acknowledges Coordination for the Improvement of Higher Education Personnel (CAPES) for the scholarship.

Appendix A. Supplementary material

Supplementary data associated with this article can be found, in the online version, at http://dx.doi.org/10.1016/j.compag.2017.12.029.

References

Ai, F.-F., Bin, J., Zhang, Z.-M., Huang, J.-H., Wang, J.-B., Liang, Y.-Z., Yu, L., Yang, Z.-Y., 2014. Application of random forests to select premium quality vegetable oils by their fatty acid composition. Food Chem. 143, 472–478.

Antonelli, A., Cocchi, M., Fava, P., Foca, G., Franchini, G.C., Manzini, D., Ulrici, A., 2004. Automated evaluation of food colour by means of multivariate image analysis coupled to a wavelet-based classification algorithm. Anal. Chim. Acta 515, 3–13.

AOAC, 2005. Official Methods of Analysis of the Association of Analytical Chemists International, 18th ed. Gathersburg, MD, USA, Official Methods.

Barbon, A.P.A., Barbon, S., Mantovani, R.G., Fuzyi, E.M., Peres, L.M., Bridi, A.M., 2016. Storage time prediction of pork by computational intelligence. Comp. Electron. Agricult. 127, 368–375.

Benassi, M.D.T., Antunes, A.J., 1988. A comparison of metaphosphoric and oxalic acids as extractants solutions for the determination of vitamin c in selected vegetables. Arquivos de Biologia e Tecnologia Instituto de Biologia e Pesquisas Tecnológicas 31, 507–513.

Blankenship, S., Unrath, C., 1988. Internal ethylene levels and maturity of delicious and golden delicious apples destined for prompt consumption. J. Am. Soc. Horticult. Sci. 113, 88–91.

Breiman, L., 2001. Random forests. Mach. Learn. 45, 5–32.

Bron, I.U., Jacomino, A.P., 2006. Ripening and quality of golden papaya fruit harvested at different maturity stages. Brazil. J. Plant Physiol. 18, 389–396.

Chen, K., Sun, X., Qin, C., Tang, X., 2010. Color grading of beef fat by using computer vision and support vector machine. Comp. Electron. Agricult. 70, 27–32.

da Costa Barbon, A.P.A., Barbon, S., Campos, G.F.C., Seixas, J.L., Peres, L.M., Mastelini, S.M., Andreo, N., Ulrici, A., Bridi, A.M., 2017. Development of a flexible computer vision system for marbling classification. Comp. Electron. Agricult. 142, 536–544.

Damez, J.-L., Clerjon, S., 2008. Meat quality assessment using biophysical methods related to meat structure. Meat Sci. 80, 132–149.

Eyarkai Nambi, V., Thangavel, K., Shahir, S., Thirupathi, V., 2016. Comparison of various RGB image features for nondestructive prediction of ripening quality of alphonso mangoes for easy adoptability in machine vision applications: a multivariate approach. J. Food Qual. 39, 816–825.

Faostat, F., 2016. Agriculture Organization of the United Nations Statistics Division. Production < http://faostat3.fao.org/browse/Q/QC/S > .

Garrido-Novell, C., Pérez-Marin, D., Amigo, J.M., Fernández-Novales, J., Guerrero, J.E., Garrido-Varo, A., 2012. Grading and color evolution of apples using RGB and hyperspectral imaging vision cameras. J. Food Eng. 113, 281–288.

Granitto, P.M., Gasperi, F., Biasioli, F., Trainotti, E., Furlanello, C., 2007. Modern data mining tools in descriptive sensory analysis: a case study with a random forest approach. Food Qual. Prefer. 18, 681–689.

Jackman, P., Sun, D.-W., ElMasry, G., 2012. Robust colour calibration of an imaging system using a colour space transform and advanced regression modelling. Meat Sci. 91, 402–407.

Kang, S., East, A., Trujillo, F., 2008. Colour vision system evaluation of bicolour fruit: a case study with b74 mango. Postharv. Biol. Technol. 49, 77–85.

Kennard, R.W., Stone, L.A., 1969. Computer aided design of experiments. Technometrics 11, 137–148.

Kim, H., Hewett, E., Lallu, N., 1999. The role of ethylene in kiwifruit softening. In: IV International Symposium on Kiwifruit, ISHS Acta Horticulturae, vol. 498, pp. 255–262.

Liu, M., Wang, M., Wang, J., Li, D., 2013. Comparison of random forest, support vector machine and back propagation neural network for electronic tongue data classification: application to the recognition of orange beverage and chinese vinegar. Sens. Actuat. B: Chem. 177, 970–980.

Magwaza, L.S., Opara, U.L., 2015. Analytical methods for determination of sugars and sweetness of horticultural products?a review. Scientia Horticulturae 184, 179–192.

Menze, B.H., Kelm, B.M., Masuch, R., Himmelreich, U., Bachert, P., Petrich, W., Hamprecht, F.A., 2009. A comparison of random forest and its gini importance with standard chemometric methods for the feature selection and classification of spectral data. BMC Bioinf. 10, 213.

Muñoz, I., Rubio-Celorio, M., Garcia-Gil, N., Guàrdia, M.D., Fulladosa, E., 2015. Computer image analysis as a tool for classifying marbling: a case study in dry-cured ham. J. Food Eng. 166, 148–155.

Nagle, M., Intani, K., Romano, G., Mahayothee, B., Sardsud, V., Müller, J., 2016. Determination of surface color of all yellow mango cultivars using computer vision. Int. J. Agricult. Biol. Eng. 9, 42.

Obledo-Vazquez, E.N., Cervantes-Martínez, J., 2017a. Laser-induced fluorescence spectral analysis of papaya fruits at different stages of ripening. Appl. Opt. 56, 1753–1756.

Obledo-Vazquez, E.N., Cervantes-Martínez, J., 2017b. Quality, bioactive compounds and antioxidant capacity of selected climacteric fruits with relation to their maturity. Scientia Horticulturae 221, 33–42.

O'Sullivan, M., Byrne, D., Martens, H., Gidskehaug, L., Andersen, H., Martens, M., 2003. Evaluation of pork colour: prediction of visual sensory quality of meat from instrumental and computer vision methods of colour analysis. Meat Sci. 65, 909–918.

Papadopoulou, O.S., Panagou, E.Z., Mohareb, F.R., Nychas, G.-J.E., 2013. Sensory and microbiological quality assessment of beef fillets using a portable electronic nose in tandem with support vector machine analysis. Food Res. Int. 50, 241–249.

Payne, A.B., Walsh, K.B., Subedi, P., Jarvis, D., 2013. Estimation of mango crop yield using image analysis–segmentation method. Comp. Electron. Agricult. 91, 57–64.

Prevolnik, M., Andronikov, D., Žlender, B., i Furnols, M.F., Novič, M., Škorjanc, D., Čandek-Potokar, M., 2014. Classification of dry-cured hams according to the maturation time using near infrared spectra and artificial neural networks. Meat Sci. 96, 14–20.

Rodriguez-Amay, D.B., 2001. A Guide to Carotenoid Analysis in Foods. ILSI Press, Washington, DC.

Rojas-Moraleda, R., Valous, N.A., Gowen, A., Esquerre, C., Härtel, S., Salinas, L., O'Donnell, C., 2016. A frame-based ANN for classification of hyperspectral images: assessment of mechanical damage in mushrooms. Neural Comput. Appl. 28, 969–981.

Ropodi, A., Panagou, E., Nychas, G.-J., 2016. Data mining derived from food analyses using non-invasive/non-destructive analytical techniques; determination of food authenticity, quality & safety in tandem with computer science disciplines. Trends Food Sci. Technol. 50, 11–25.

Savakar, D.G., Anami, B.S., 2015. Grading of bulk food grains and fruits using computer vision. J. Agricult. Eng. Biotechnol. 3, 1–10.

Valous, N., Zheng, L., Sun, D.-W., Tan, J., 2016. Quality evaluation of meat cuts. In: Computer Vision Technology for Food Quality Evaluation, second ed. Elsevier, pp. 175–193.

Valous, N.A., Mendoza, F., Sun, D.-W., Allen, P., 2010. Supervised neural network classification of pre-sliced cooked pork ham images using quaternionic singular values. Meat Sci. 84, 422–430.

Vélez-Rivera, N., Blasco, J., Chanona-Pérez, J., Calderón-Domínguez, G., de Jesús Perea-Flores, M., Arzate-Vázquez, I., Cubero, S., Farrera-Rebollo, R., 2014. Computer vision system applied to classification of manila mangoes during ripening process. Food Bioproc. Technol. 7, 1183–1194.

Wang, D., Wang, X., Liu, T., Liu, Y., 2012. Prediction of total viable counts on chilled pork using an electronic nose combined with support vector machine. Meat Sci. 90, 373–377.

Wu, D., Sun, D.-W., 2013. Colour measurements by computer vision for food quality control–a review. Trends Food Sci. Technol. 29, 5–20.

Zhang, C., Liu, C., Zhang, X., Almpanidis, G., 2017. An up-to-date comparison of state-of-the-art classification algorithms. Expert Syst. Appl. 82, 128–150.

Zhou, L., Paull, R.E., 2001. Sucrose metabolism during papaya (carica papaya) fruit growth and ripening. J. Am. Soc. Horticult. Sci. 126, 351–357.